CI&CEQ
Chemical Industry & Chemical Engineering Quarterly

Available on line at
Association of the Chemical Engineers of Serbia AChE
www.ache.org.rs/CICEQ

Chem. Ind. Chem. Eng. Q. 27 (3) 223–230 (2021) CI&CEQ

NAVEEDUL HASAN SYED[1]
NASEER AHMED KHAN[1]
IFTIKHAR AHMAD[2]

[1]Department of Chemical Engineering, University of Engineering and Technology Peshawar, Pakistan
[2]Department of Chemical Engineering, National University of Sciences and Technology Peshawar, Pakistan

SCIENTIFIC PAPER

UDC 66.096.5:66

A COMPUTATIONAL STUDY OF A MULTI-SOLID-LIQUID FLUIDIZED BED INCORPORATING INCLINED CHANNELS

Article Highlights

- The reflux classifier with wide channel spacing is simulated using 2D continuum model
- A coal feed comprising solid particles with different densities and sizes is used
- The segregation of solid particles was based on difference in their densities
- Total and individual solid concentrations are illustrated within the device
- Suspension density within the fluidization section of the device is shown

Abstract

Simulations were performed under continuous processing conditions using the 2D continuum model to describe the internal state of a multi-solid system, comprising solid particles of different sizes and densities at the same time. The feed consisted of 35 types of solid particle species with five different sizes, 1.70, 1.20, 0.85, 0.60 and 0.35 mm, and seven different densities ranging from 1400 to 2000 kg/m^3. The simulations results have been used to plot the concentration profiles of solid particles along the bed height. The concentration profiles of the solid particles depicted that the fine dense particles, 0.60 mm, having density equal to 1900 kg/m^3 and terminal velocity 0.058 m/s moved downwards and discharged into the underflow. However, the low-density coarse particles, 1.20 mm, having density equal to 1400 kg/m^3 and terminal velocity 0.068 m/s moved upwards and conveyed to the overflow, hence, show a separation process based on the density difference. Furthermore, simulation results showed that the particle species having densities close to the value of the separation relative density exhibited higher concentrations along the system height, and the suspension within the system was mainly composed of these species.

Keywords: density separation, fluidization, multiphase flow, polydisperse suspension, segregation-dispersion model, simulations.

Liquid fluidized bed (LFB) separators including teeter bed separators and the Reflux Classifier™, have a wide range of applications in mineral processing, bio-solubilization of coal, catalytic cracking, and gas purification [1-4]. The Reflux Classifier™, developed by Galvin and in his co-workers in 2001 [4,5], is a novel beneficiation technology and has opened new areas of research since its invention. The Reflux Classifier™ consists of a fluidization (vertical) section and an inclined section above it [4], Figure 1. The inclined section consists of a set of parallel inclined plates, which work on the principle of the Boycott effect [6]. According to the Boycott effect [6], the inclined channels provide a large settling area and enable the particle species to settle at a relatively fast rate as compared to the vertical channels. Thus, the fine dense particle species that escape from the fluidization section of the Reflux Classifier™ get another chance to settle onto the inclined channels and slide back towards the fluidization section and discharge in the underflow, whereas the fine low-density particles remain in suspension within the inclined channel and move out via the overflow. The configuration of the device can be found as wide channel spacing (chan-

Correspondence: N.H. Syed, Department of Chemical Engineering, University of Engineering and Technology Peshawar Pakistan.
E-mail: syednaveed@uetpeshawar.edu.pk
Paper received: 29 May, 2020
Paper revised: 28 August, 2020
Paper accepted: 26 October, 2020

https://doi.org/10.2298/CICEQ200529041S

nel spacing >6 mm) [7,9] and narrow channel spacing (channel spacing ≤6 mm) [3] inclined channels.

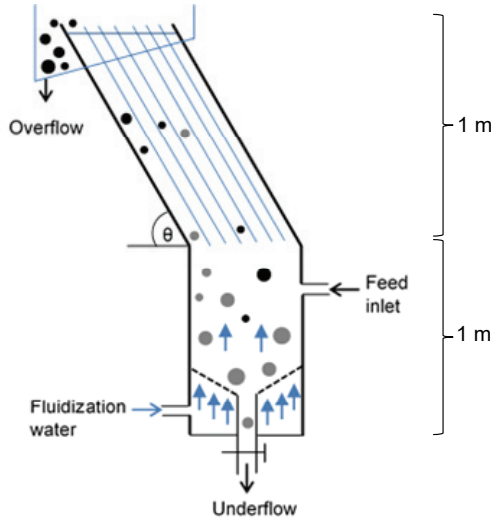

Figure 1. Schematic representation of the Reflux Classifier, a fluidized bed incorporating inclined channels.

Many laboratory-, pilot-scale and full plant-scale developments and research studies have been carried out on the Reflux Classifier™ to separate valuable minerals, such as coal and iron ore from gangue [3,5,7,8,10]. The device has progressed as an excellent gravity separation device [3,10], offering three times higher throughput advantage over the conventional liquid fluidized bed separators [5]. In the first pilot plant trial [5], the device was used to separate coal particles of size -2+0.125 mm at high solids loading of 47 t/m^{2}h, which was a significantly higher throughput than for a teeter bed separator [5]. Moreover, the partition curves produced from the experimental data showed better separation performance of the device with less variation in the D_{50} and the separation efficiency values with changing particle size [5,7].

Similarly, some computational studies were also performed by different researchers on the Reflux Classifier™, such as in 2005, when Doroodchi *et al.* [11] examined the influence of inclined plates on the expansion behavior of mono and binary mixtures using a CFX 5.6 code. Recently, Peng *et al.* [12] utilized a coupled CFD and DEM approach to study the segregation of solid particles within the Reflux Classifier.

Nevertheless, in contrast to the experimental studies, the computational studies performed on the Reflux Classifier™ were few in number. Contrary to the Reflux Classifier™, extensive computational studies have been performed to describe transport mechanism of solid particles species in conventional liquid fluidized devices, *i.e.*, teeter bed separators [13-22]. However, the computational studies performed on liquid fluidized beds and more specifically on the Reflux Classifier™ were related to the systems operated under batch process conditions, and the studies focusing on the continuous fluidization processes with multicomponent species were sparse.

The computational studies can be utilized to fully understand the mechanism of particle transport in a fluidization process. The continuous fluidization processes, handling multicomponent species and representing the industrial operations, are more complex and difficult to study. The understanding of such systems is vital for efficient design, operations, and scale-up of the devices and to provide a comprehensive knowledge of the transport behavior of solid particles.

Syed *et al.* [9,23] provided a comprehensive 2D continuum model based on Kennedy and Bretton [16] approach for the Reflux Classifier™ operated under continuous process conditions. The authors, in 2016 [9], successfully validated predictions of the 2D continuum model with the published experimental results of Galvin *et al.* [7] obtained from a Reflux Classifier™ with wide channel spacing. Subsequently, Syed *et al.* [23] modeled the Reflux Classifier™ with narrow channel spacing using 2D continuum model and validated the model predictions with the experimental results of Galvin *et al.* [3].

The present study is an extension of the work of Syed *et al.* [9]. This work is significant as the internal state of a complex multi-solid system [9] comprising particle species with different sizes and densities at the same time in the Reflux Classifier™ is demonstrated for the first time using the 2D continuum model. The model has been used to describe segregation of solid particles based on density differences under continuous process conditions for a case when the Reflux Classifier was run on a full-scale in 2005. The results have been used to illustrate total and individual solid concentration profiles, concentration profiles of the particles of specific size range contributing towards total solid concentration, suspension density and presence of D_{50} particles as a major part of the suspension within the device.

2D CONTINUUM MODEL

The 2D continuum model is based on the Kennedy and Bretton [16] approach, and states that in a modified fluidized bed separator incorporating inclined channels above it, the net flux of a particle species relative to the vessel is the sum of dispersion and

segregation fluxes having x and y components [9,23] given as:

$$J_{x,i} = C_i u_{p\_x,i} = -D_{x,i}\frac{\partial C_i}{\partial x} + C_i u_{sg\_x,i} \quad (1)$$

$$J_{y,i} = C_i u_{p\_y,i} = -D_{y,i}\frac{\partial C_i}{\partial y} + C_i u_{sg\_y,i} \quad (2)$$

where J_x, J_y, u_{p_x} and u_{p_y} are x (horizontal) and y (axial) components of the net flux and particle velocity relative to the vessel, respectively. Similarly, u_{sg_xi}, u_{sg_yi}, D_{xi}, D_{yi}, C_i, $-D_{x,i}\partial C_i/\partial x$, $-D_{y,i}\partial C_i/\partial y$, $C_i u_{p\_x,i}$ and $C_i u_{p\_y,i}$ are the segregation velocity, dispersion coefficient, solid concentration, dispersion flux and segregation flux in the horizontal and axial directions for solid particle species i, respectively.

In a continuous process, there is a flow coming into the system as a feed and going out as an underflow and overflow. The total-volume flux, V_n, through the system at feed inlet and just above the feed inlet is given as [9]:

$$V_n = u_{fs} + J_f - J_u = u_f\varepsilon_f + \sum C_i u_{p,i} \quad (3)$$

Now the total-volume flux below the feed inlet [9] is given as:

$$V_n = u_{fs} - J_u = u_f\varepsilon_f + \sum C_i u_{p,i} \quad (4)$$

where u_{fs} is the superficial fluidization velocity, u_f the interstitial fluid velocity, J_f is the feed flux, J_u is the underflow flux and ε_f is the voidage.

The 2D continuum model was solved by a set of algebraic equations. The complete algorithm of the model is provided by Syed *et al.* [9]; however, a brief summary is given in this paper.

The segregation velocity in the horizontal and axial direction is calculated as:

$$u_{sg\_x,i} = u_{slip\_x,i} + u_{f,x} \quad (5)$$

$$u_{sg\_y,i} = u_{slip\_y,i} + u_{f,y} \quad (6)$$

where $u_{sg\_x,i}$ and $u_{f,x}$ are the slip velocity of the particle species relative to the fluid and interstitial fluid velocity in the horizontal direction, respectively. Likewise, $u_{slip\_y,i}$ and $u_{f,y}$ are the slip velocity of the particle species relative to the fluid and interstitial fluid velocity in the axial direction, respectively.

The horizontal and axial components of the slip velocity were calculated by incorporating the hindered settling model of Asif [17], in the 2D continuum model, given as:

$$u_{slip,i} = u_{t,i}\left(\frac{\rho_i - \rho_{sus}}{\rho_i - \rho_f}\right)^{n_i - 1} \quad (7)$$

In the hindered settling model, the empirical exponent was applied as an absolute value of the normalized density difference to obtain the hindered settling factor, $((\rho_i - \rho_{sus})/(\rho_i - \rho_f)^{n_i-1}$, by introducing a directional parameter, ℓ, [9,23]. The directional parameter, $\ell = 1$, if $((\rho_i - \rho_{sus})/(\rho_i - \rho_f)$ is greater than or equal to zero, and $\ell = -1$, if $((\rho_i - \rho_{sus})/(\rho_i - \rho_f)$ is less than zero. Now, the slip velocity model in the horizontal and axial directions becomes:

$$u_{slip\_x,i} = \left[u_{t,i}\,\ell\left|\left(\frac{\rho_i - \rho_{sus}}{\rho_i - \rho_f}\right)\right|^{n_i-1}\right]\cos\theta \quad (8)$$

$$u_{slip\_y,i} = \left[u_{t,i}\,\ell\left|\left(\frac{\rho_i - \rho_{sus}}{\rho_i - \rho_f}\right)\right|^{n_i-1}\right]\sin\theta \quad (9)$$

where ρ_i, ρ_f and ρ_{sus} are the density of the particle species i, the fluid density and the suspension density, respectively. The suspension density, ρ_{sus}, is given as:

$$\rho_{sus} = \sum C_i\rho_i + (1 - \sum C_i)\rho_f \quad (10)$$

At steady state, the interstitial fluid velocity within the fluidization section is quantified using Eqs. (3) and (4). Similarly, the interstitial fluid velocity within the inclined channel in horizontal and axial direction is calculated using the net flux equations in the corresponding directions.

The dispersion flux is quantified using fixed values of the dispersion coefficient, *i.e.*, 0.0030 and 0.00030 m^2/s, in the fluidization and inclined sections of the device [23].

The boundary conditions at the top and base of the system are given as:

$$y = y_{max},\ \frac{\partial C_i}{\partial y} = 0 \quad (11)$$

$$y = 0,\ J_{y,i} = J_u \quad (12)$$

Continuum model implementation and the computational domain

The computational domain of the Reflux Classifier was discretized into 100 shells and 11 elements in the axial and horizontal directions, respectively. Figure 2 shows the computational geometry of the Reflux Classifier. The process conditions for running simulations were selected as were used by Galvin *et al.* [7]. The authors [7] used a feed comprising particle size range -2.0+1.40 mm, -1.40+1.0 mm, -1.0+0.70 mm, -0.70+0.50 mm and -0.50+0.25 mm in the Reflux Classifier. In order to represent the actual feed in simulations, a total 35 types of solid particle species

with 7 densities ranging 1400-2000 kg/m^3 and 5 different sizes with average particle size, *i.e.*, 1.70, 1.20, 0.85, 0.60 and 0.35 mm, were selected for the corresponding particle size range. Likewise, the feed slurry containing solids and liquid was taken as total solid-flux equal to 0.0040 m^3/(m^2 s) and water-flux equal to 0.012 m^3/(m^2 s). The fluidization velocity and the underflow rate were kept at 0.0050 and 0.0040 m^3/(m^2 s). The underflow rate value was set in a way to obtain the D_{50} values as were obtained in the experiments by Galvin *et al.* [7]. The types and properties of the solid particle species selected in this study are tabulated in supplementary Table A.1 (available from the author upon request).

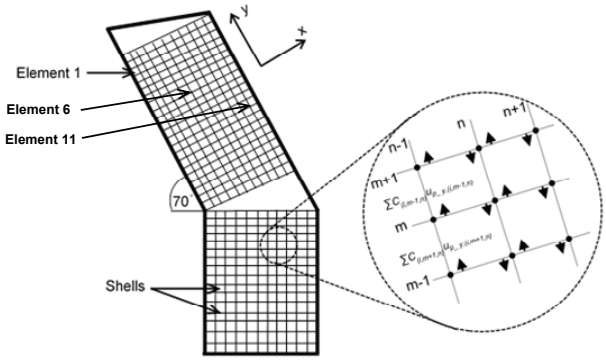

Figure 2. A representation of the computational domain of the Reflux Classifier with magnified view of the mesh demonstrating flux movement.

Separation relative density

A partition curve indicates the percentage of entrainment for each relative density or size fraction in a product stream (overflow) or the reject stream (underflow) after separation. The separation density cut point or separation relative density, D_{50}, represents the relative density of solid particle species that have a 50% probability to report either to the underflow or overflow. Similarly, the D_{25} and D_{75} indicate the relative density of solid particle species that have 25 and 75% probability to report to the overflow, respectively, Figure 3.

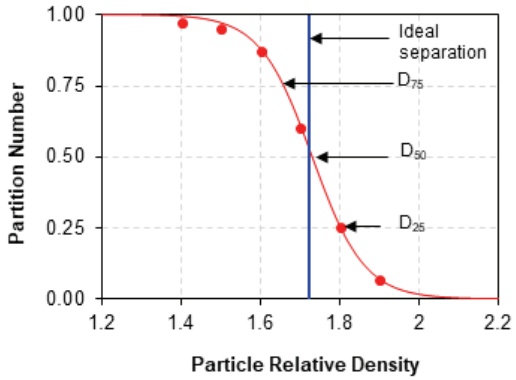

Figure 3. Illustration of D_{50} and partition curve.

RESULTS AND DISCUSSION

Total solid concentration profiles

Simulation data were used to obtain the separation relative density, D_{50}, values for each particle size range matched. The D_{50} values matched well with the experimental results of Galvin *et al.* [7], Table 1. The results show that the D_{50} values increased with the decreasing particle size, as was observed experimentally by Galvin *et al.* [7]. The particle species whose relative densities/densities were equal to the D_{50} values or whose relative densities/densities were close to the D_{50} values had 50 % probability to move out from the system either in the overflow or in the underflow. These species are termed as the species behaving as the D_{50} particles and were anticipated to form the main suspension within the system.

Figure 4 shows the profiles of the total solid concentration as a function of system height for the validated results by Syed *et al.* [9] in elements 1, 6 and 11. The model predictions show that the system achieved a maximum solid volumetric concentration of 0.60 near the base. The concentration gradually decreased along with the system height. Within the inclined channel, the system achieved a maximum concentration of 0.37 (at 1.50 m height) in element 1. The results show that the total concentration of the solid particles remained the same in the fluidization section in all elements, whereas, variations in the total

Table 1. Comparison of the D_{50} values for the given particle size range

Particle size range (mm)	Average particle size (mm)	D_{50} obtained from the experimental work (Galvin *et al.* [21])	D_{50} obtained from simulations
-2.0 +1.40	1.70	1.46	1.45
-1.40 +1.0	1.20	1.53	1.51
-1.0 +0.70	0.85	1.62	1.59
-0.70 +0.50	0.60	1.74	1.73
-0.50 +0.25	0.35	1.94	2.03

concentration were observed within the inclined channel. The total concentration of the solid particles decreased with an increase in element number across the channel width. The solid concentration of 0.37 at a height of 1.50 m in element 1 reduced from 0.37 to 0.34 and to 0.28 in elements 6 and 11, respectively. This is because solid particles, after entering the inclined channel, settled onto the upward-facing wall of the channel relatively at a high rate due to large settling area provided by the inclined channel. The concentration of solid particles hence increased on the upward facing wall of the channel, *i.e.*, in element 1, as compared to the middle and upper zones across the channel width, *i.e.*, in elements 6 and 11. These particles after settling slide back towards the fluidization section and are discharged into the underflow.

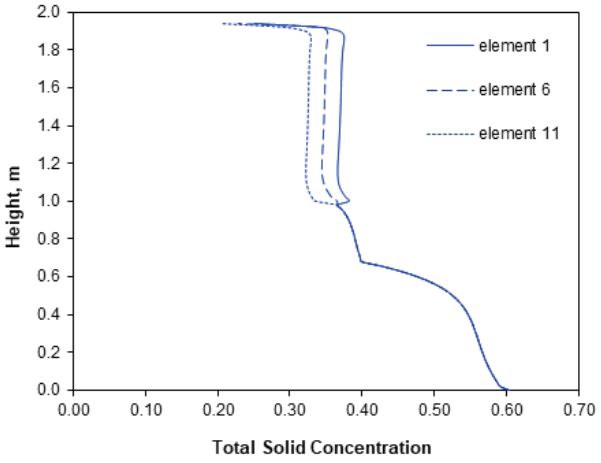

Figure 4. Total solid concentration versus height in elements 1, 6 and 11.

Individual solid concentration profiles

Figure 5a and b show profiles of individual solid concentration in the selected size ranges within the fluidization and inclined sections of the system in element 1. In this study, 35 different types of solid particle species were used, so there were complex and scattered concentration profiles of solid particles which could distract the readers. Therefore, concentration profiles in the selected particle size ranges are shown here to minimize the noise.

Figure 5a shows the individual concentration profiles of solid particle species for the average particle size 0.60 mm versus height in element 1. Figure 5a illustrates that the denser species (1800, 1900, and 2000 kg/m^3) had higher concentrations near the base of the system and lower concentrations above the feed inlet and within the inclined section of the system. The denser species discharged in the underflow. On the contrary, the low-density species (1400, 1500 and 1600 kg/m^3) exhibited relatively high concentrations in the inclined section and low concentrations in the fluidization section of the system. These species, due to low density, move upwards and are collected as a top product. For instance, particle species with a density equal to 2000 kg/m^3 achieved a maximum solid concentration of 0.028 at the base of the system. Its concentration decreased with elevation and was almost zero within the inclined section. In contrast, the particle species with a density equal to 1400 kg/m^3 had a lower concentration near the base, *i.e.*, almost zero, but gradually increased with the elevation. Within the inclined section, these species had a maximum concentration of 0.0062 at a height of 1.60 m (shell 60). Furthermore, the particle species with density equal to 1700 kg/m^3, curve with

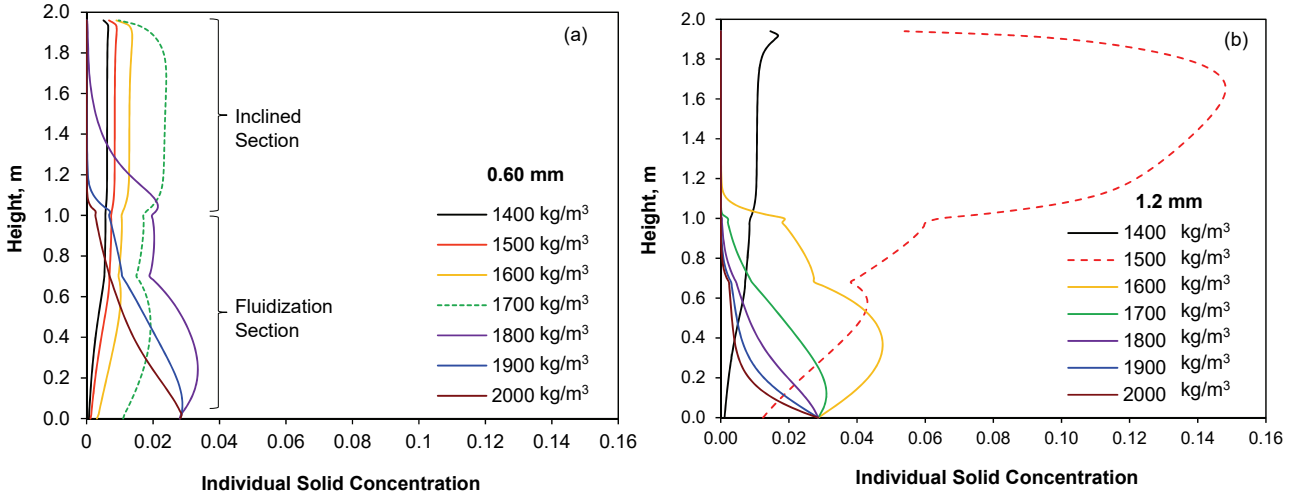

Figure 5. Individual solid concentrations of the particle species versus height: a) concentrations of particle species of size 0.60 mm; b) concentration of particle species of size 1.2 mm.

green dashed lines, exhibited their presence in both sections of the device. The relative separation density or the D_{50} value for the average particle size of 0.60 mm was 1.74, refer to Table 1 and supplementary Figure A-1. As there was no species with relative density exactly equal to 1.74 in the simulations, so the particle species with relative density equal to 1.70 (1700 kg/m^3), behaved as the D_{50} particles for the average particle size range 0.60 mm and showed their presence in the fluidization and inclined sections of the system. The D_{50} value shows that for the average particle size range 0.60 mm, the particle species with relative density/density greater than the D_{50} value discharged from the base, whereas, the ones with lower relative density/density than the D_{50} values move out *via* the overflow.

Figure 5b shows profiles of individual solid concentration of particle species for the average particle size 1.20 mm versus height in element 1. The figure illustrates that the particle species with densities equal to 1600 kg/m^3 and higher discharged into the underflow, as being coarser and having high settling velocities. Whereas, the particle species having a density equal to 1400 kg/m^3 showed their presence within the inclined section and moved out *via* the overflow. The particle species, 1500 kg/m^3, exhibited their presence in both sections of the device. These particles behaved as the D_{50} particles, because the relative density of these species, *i.e.*, 1.50, was close to the D_{50} value of 1.51, Table 1.

It is evident in Figure 4 that the 2D continuum model accurately described the transport behaviour of solid particle species based on density differences. The figure shows that after segregation, there was a higher solid concentration near the base as compared to the middle and inclined sections of the device. The higher solid concentration created an autogenous dense medium that caused high interstitial fluid velocity near the base of the device, thus only the densest and coarsest particles could enter that region, whereas the lighter ones were pushed upwards. For instance, in Figure 5a the particle species with a size equal to 0.60 mm (fine size) and density 1900 kg/m^3 had a terminal velocity of 0.058 m/s. These species moved downwards and discharged into the underflow. Nevertheless, the particle species of size 1.20 mm and density equal to 1400 kg/m^3, Figure 5b, with a higher terminal settling velocity of 0.068 m/s, moved upwards and conveyed to the overflow.

Figure 6 shows the concentration profiles of solid particles in the selected size range versus height in element 1. The figure shows the contribution of each size fraction towards the total solid concentration. For instance, particle species with average size 0.35 mm, had the lowest solid concentration within the system. These species achieved a maximum solid concentration of 0.027 near the base of the system, whereas within the inclined section these species had a maximum solid concentration of 0.052 at a height of 1.50 m. In contrast, the particle species with average size 1.70 mm had a higher concentration in the fluidization section of the device and achieved a maximum solid concentration of 0.17 near the base, whereas within the inclined section their presence was the lowest. However, the species with average particle size 1.20 mm exhibited their presence in both sections of the system. These species achieved a maximum solid concentration of 0.16 near the base and similarly, exhibited a concentration of 0.16 within the inclined section of the system at a height of 1.75 m.

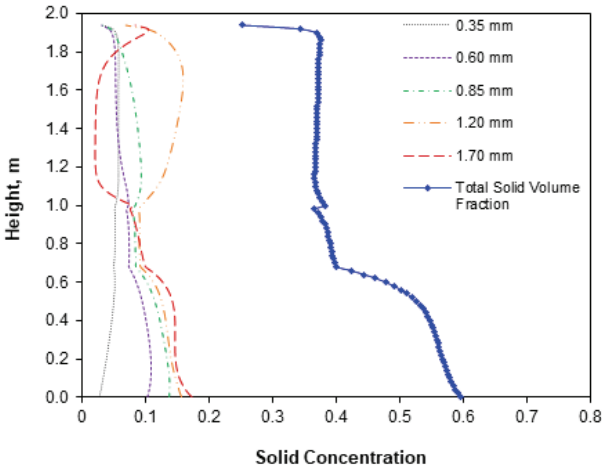

Figure 6. Profiles of solid concentration of the selected average particle size range versus height, contributing towards the total solid concentration in element 1.

Figure 7 shows a comparison between the concentrations of solid particles in the selected size range without the contribution of the concentrations of particles behaving as D_{50}, the total concentration of particle species behaving as D_{50}, and the total solid concentration versus height in element 1. The plots with dotted/dashed lines illustrate solid concentrations in the selected size range without the inclusion of the concentrations of the particle species behaving as the D_{50} particles. The model predictions show that there was a significant decrease in the solid concentrations compared to Figure 6. The profile with empty circles shows the total concentration of solid particle species behaving as D_{50} within the system, while the profile with diamonds represents the total solid concentration. The concentration profile of the D_{50} particles

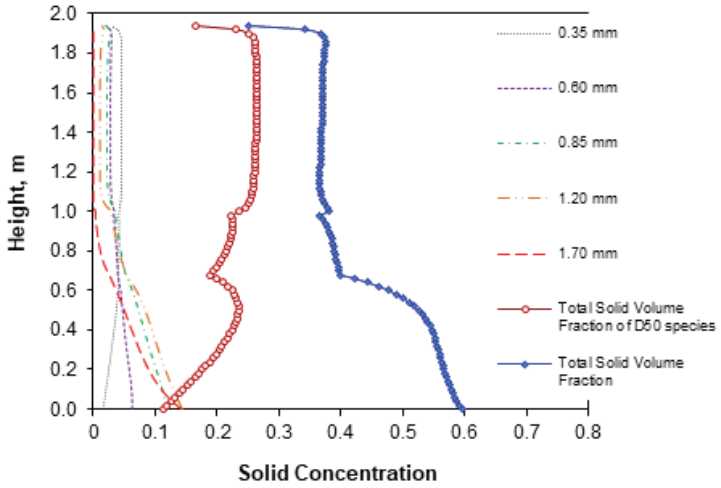

Figure 7. Comparison of the individual solid concentration of the selected average particle size range, total solid concentration of particle species behaving as the D_{50} and the overall total solid concentration of solid particles within element 1 of the computational domain of the Reflux Classifier.

depicts that these species achieved a maximum concentration of 0.11 near the base. The concentration increased gradually along the system height reaching to 0.23 and 0.26 in the middle of the fluidization and inclined sections, respectively. It is evident that these species had a higher concentration as compared to other species within the system and hence the suspension within the system was mainly composed of the D_{50} particles.

Suspension density within the fluidization section

Figure 8 represents the suspension density *versus* height in the fluidization section of the system. The suspension density had relatively higher values at the base than at the top of the fluidization section. At the base, the suspension density had a maximum value of 1465 kg/m^3 because denser particles moved downwards and settled in that region. The suspension density reduced gradually to a value of 1250 kg/m^3 near the feed inlet. In the section above the feed inlet, the suspension density decreased to a value of approximately 1235 kg/m^3, demonstrating a dilute zone due to feed (slurry) entering with water.

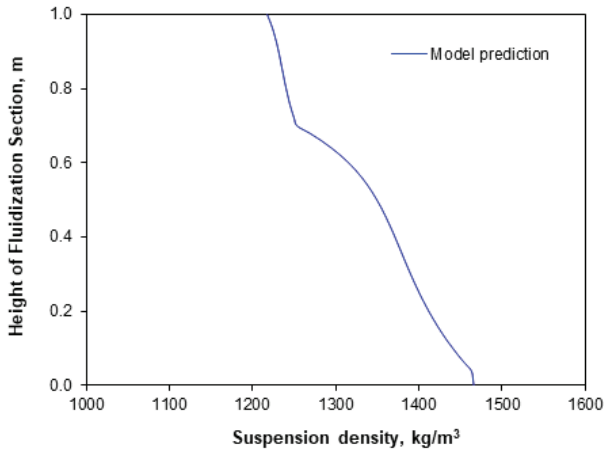

Figure 8. Suspension density versus height within the fluidization section of the Reflux Classifier.

CONCLUSIONS

A computational study was performed using the 2D continuum model to describe the internal state of a complex multi-solid system in a fluidized bed incurporating inclined channels above it under continuous processing conditions. The multi-solid system consisted of 35 types of solid particle species of five different sizes and seven different densities at the same time. The simulation results showed that solid particles were separated due to the difference in their densities. The fine dense particles having low settling velocity had a higher concentration near the base, *i.e.*, fluidization section, of the device. Whereas, the low-density coarse particle species having a higher terminal settling velocity exhibited a higher concentration in the inclined section of the device. Furthermore, the concentration profiles of the solid particle species showed that the suspension within the system was mainly composed of the particle species behaving as the D_{50}. These particles exhibited their presence in both sections of the device.

Acknowledgments

The authors greatly acknowledge the University of Newcastle Australia and Australian Government RTP scholarship for the earlier part of this PhD research topic during 2013 to 2017. The authors acknowledge the facilities provided by the Department of

Chemical Engineering, University of Engineering & Technology Peshawar, Pakistan, during this research work.

REFERENCES

[1] N. Epstein, Powder Technol. 151 (2005) 2-14

[2] R. Escudie, N. Epstein, J.R. Grace, H.T. Bi, Chem. Eng. Sci. 61 (2006) 1528-1539

[3] K.P. Galvin, J. Zhou, K. Walton, Miner. Eng. 23 (2010) 326-338

[4] G. Nguyentranlam, K.P. Galvin, Miner. Eng. 14 (2001) 1081-1091

[5] K.P. Galvin, E. Doroodchi, A.M. Callen, N. Lambert, S.J. Pratten, Miner. Eng. 15 (2002) 19- 25

[6] A.E. Boycott, Nature 104 (1920) 532

[7] K.P. Galvin, A. Callen, J. Zhou, E. Doroodchi, Miner. Eng. 18 (2005) 19-24

[8] D.M. Hunter, J. Zhou, S.M. Iveson, K.P. Galvin, Mineral Process. Extract. Metall. 125 (2016) 126-131

[9] N.H. Syed, K.P. Galvin, R. Moreno-Atanasio, in Chemeca 2016: Chemical Engineering - Regeneration, Recovery and Reinvention, Engineers Australia, Melbourne, 2016, 570-580

[10] D. Amariei, D. Michaud, G. Paquet, M. Lindsay, Miner. Eng. 62 (2014) 66-73

[11] E. Doroodchi, K.P. Galvin, D.F. Fletcher, Powder Technol. 160 (2005) 20-26

[12] Z. Peng, K.P. Galvin, E. Doroodchi, Powder Technol. 343 (2019) 170-184

[13] T.B. Anderson, R. Jackson, Ind. Eng. Chem. Fundam. 6 (1967) 527-539

[14] R.K. Reddy, J.B. Joshi, Chem. Eng. Sci. 64 (2009) 3641--3658

[15] H. Abbasfard, G.M. Evans, M.S. Khan, R. Moreno-Atanasio, Chem. Eng. Sci. 180 (2018) 79-94

[16] S.C. Kennedy, R.H. Bretton, AIChE J. 12 (1966) 24-30

[17] M. Asif, Chem. Eng. Technol. 20 (1997) 485-490

[18] M. Asif, J.N. Petersen, AIChE J. 39 (1993) 1465-1471

[19] W.F. Ramirez, K.P. Galvin, AIChE J. 51 (2005) 2103--2108

[20] M. Asif, J.N. Petersen, E.N. Kaufman, J.M. Cosgrove, T.C, Scott, Ind. Eng. Chem. Res. 33 (1994) 2151-2156

[21] B.K. Patel, W.F. Ramirez, K.P. Galvin, Chem. Eng. Sci. 63 (2008) 1415-1427

[22] Z. Peng, J.B. Joshi, B. Moghtaderi, M.S. Khan, G.M. Evans, E. Doroodchi, Chem. Eng. Sci. 152 (2016) 65-83

[23] N.H. Syed, J.E. Dickinson, K.P. Galvin, R. Moreno-Atanasio, Miner. Eng. 115 (2018) 53-67.

NAVEEDUL HASAN SYED[1]
NASEER AHMED KHAN[1]
IFTIKHAR AHMAD[2]

[1]Department of Chemical Engineering, University of Engineering and Technology Peshawar, Pakistan
[2]Department of Chemical Engineering, National University of Sciences and Technology Peshawar, Pakistan

NAUČNI RAD

KOMPJUTERSKO PROUČAVANJE FLUIDIZOVANOG SLOJA ČVRSTO-TEČNO SA ISKOŠENIM KANALIMA

Simulacije su izvedene u kontinualnim procesnim uslovima pomoću 2D modela kontinuuma da bi se istovremeno opisalo unutrašnje stanje sistema koji sadrži čvrste čestice različitih veličina i gustina. Korišćene su 35 vrsta čvrstih čestica pet različitih veličina, 1,70, 1,20, 0,85, 0,60 i 0,35 mm i sedam različitih gustina u rasponu od 1400 do 2000 kg/m^3. Rezultati simulacije korišćeni su za crtanje profila koncentracije čvrstih čestica po visini sloja. Profili koncentracija čvrstih čestica otkrili su da se fine guste čestice, veličine 0,60 mm, gustine 1900 kg/m^3 i terminalne brzine 0,058 m/s pomeraju nadole i ispuštaju u podtok. Međutim, krupnije čestice, veličine 1,20 mm, gustine 1400 kg/m^3 i terminalne brzine 0,068 m/s, pomerile su se nagore i odnošene u preliv, što pokazuje proces razdvajanja zasnovan na razlici gustine. Dalje, rezultati simulacije pokazali su da su vrste čestica sa gustinama koje su blizu vrednosti relativne gustine razdvajanja bile u većoj koncentraciji duž visine sistema, dok je suspenzija unutar sistema bila sastavljena uglavnom je od ovih čestica.

Ključne reči: separacija na bazi gustine, fluidizacija, višefazni tok, polidisperzna suspenzija, segregaciono-disperzioni model, simulacije.